Progress In Electromagnetics Research C, Vol. 173, 207–214, 2026

(Received 14 July 2026, Accepted 26 August 2026, Scheduled 11 September 2026)

A Compact Multilayer Quad-Band Bandpass Filter with Coupled SIRs for Multi-Standard Wireless Systems

Hassan S. Abdullah* and Raaed T. Hammed

Department of Electrical Engineering, University of Technology — Iraq, Baghdad, Iraq

ABSTRACT: In this paper, we propose a compact quad-band bandpass filter by using short-ended stepped-impedance resonators (SE-SIRs) and open-ended stepped-impedance resonators (OE-SIRs) in a hybrid structure. The proposed design uses the odd- and even-mode resonances of the two types of resonators to produce four independent passbands in a compact multilayer structure. The first and second passbands are set by SE-SIR resonators at 1.56 and 2.5 GHz, respectively. The third and fourth passbands are centered at 3.5 and 5.2 GHz, respectively, due to the OE-SIR resonators. To achieve the quad-band response in a compact size, a multilayer arrangement with electromagnetic broadside coupling between the feeding structure and resonators has been adopted. Finally, the filter is designed, simulated, fabricated, and measured using a Rogers-Ceramic RO4360 substrate with a permittivity of $\varepsilon_r = 6.15$ and thicknesses of $(h_1 = 0.3, h_2 = 0.508)$ mm. Simulated insertion losses were 0.29, 0.26, 0.43, and 0.66 dB, and return losses were 28.65, 15.05, 1404, and 173 dB in each of the four operating bands, respectively. Filter responses from simulation and measurement are contrasted and discussed. The produced filter is very small, covering a circuit area of about 129 mm², without feeding ports.

1. INTRODUCTION

The rapid growth of wireless communication networks has increased the demand for small multiband bandpass filters with high performance, low insertion loss, excellent selectivity, and spectral efficiency. Stepped-impedance resonator (SIR) is one of the most attractive filter design methods because of their compact size, ability to tune the resonant frequency by varying dimensions and generating multiple resonant modes. Integrating open stubs with SIR structures can achieve high-frequency and ultra-wideband filtering responses while maintaining simple geometric shapes [1]. Later, embedded and stub-loaded SIR structures were proposed for compact multiband operation with triple-band responses and enhanced frequency selectivity [2]. Moreover, dual-mode bandpass filters with good selectivity improvement have been designed using symmetrical T-shaped stub-loaded SIRs by generating transmission zeros [3]. The increasing need for dual- and multiband wireless devices has resulted in many filter designs for various communication protocols. Some tiny dual-band bandpass filters have been reported based on cross-coupled dual-mode isosceles right-angled triangular (IRAT) resonators, where coupling between LC and cavity modes can provide a large number of transmission zeros and good selectivity [4]. Other studies have investigated using small Global System for Mobile Communications (GSM)/Global Positioning System (GPS) filtering structures with T-shaped resonators and wide-stopband dual-band filters for improved stopband performance and size reduction [5, 6]. Similarly, dual-band bandpass filters based on Grounded Stepped-Impedance Resonator (GSIR) using electrically coupled ring-shaped stubs have been shown to have compact dimensions, low insertion loss, and ultra-wide stopband suppression, substantially improving filtering selectivity [7]. Recently, advanced resonator technologies have been reported that provide improved electrical performance and greater operational flexibility, including switchable low-loss filtering structures, closely spaced dual-band responses, and layered spherical resonators [8–11]. In addition to supporting multi-band operation, modern wireless communication systems require filters with high frequency selectivity and narrow passband characteristics. Thus, much effort has been devoted to dual-band filtering solutions such as ultra-narrowband filters for WiMAX applications, large-bandwidth-ratio millimeter-wave filters, and wideband dual-band configurations using different substrate technologies [12–14]. In addition, independently tunable passbands and reconfigurable dual-band filter architectures are proposed to improve frequency selectivit, providing increased operational flexibility. Passbands and reconfigurable dual-band filter architectures have been proposed to improve frequency selectivity while increasing operation flexibility and maintaining desirable bandwidth characteristics [15, 16]. Multilayer and dual-mode technologies have attracted considerable attention recently because of their ability to overcome the limitations of planar architectures. Multilayer dual-mode resonator topologies with interlayer electromagnetic coupling have been used to obtain small dual-band filters with improved filtering performance and multiple transmission zeros [17]. Likewise, multilayer filtering approaches have been of interest for enhancing compactness and spectrum selectivity. Multilayer dual-mode resonators and microstrip-to-slotline transition-based dual-band filters have low loss, im-

* Corresponding author: Hassan Saad Abdullah (hassan.s.abdullah@uotechnology.edu.iq).

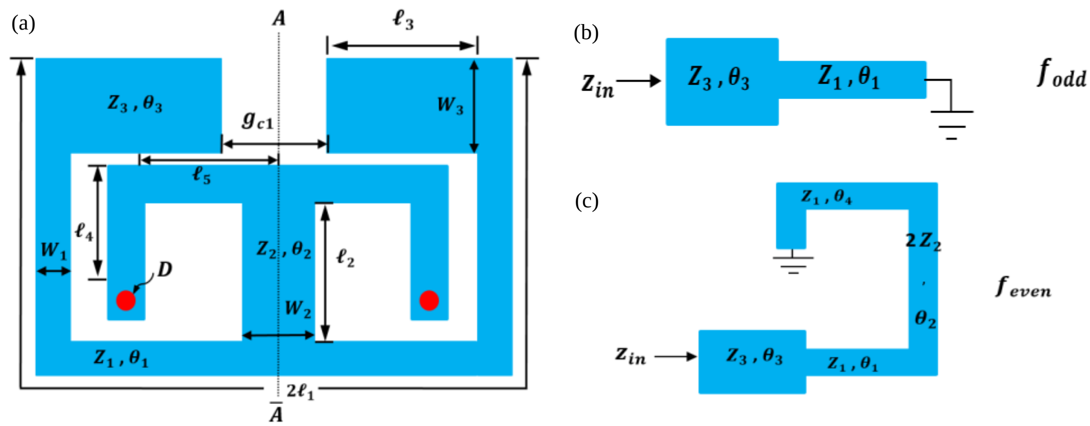

FIGURE 1. Proposed short-ended stepped-impedance resonator (SE-SIR): (a) Physical configuration, (b) odd-mode equivalent circuit, and (c) even-mode equivalent circuit.

proved interband isolation, and multiple transmission zeros, making them suitable for tiny multiband microwave frontend systems [18, 19]. Therefore, in this study, a small multilayer bandpass filter based on coupled stepped-impedance resonators (SIRs) and broadside-coupled transmission lines is proposed. The proposed structure is based on multilayer electromagnetic coupling and operates at 1.56, 2.5, 3.5, and 5.2 GHz while maintaining its compactness and high filtering performance. Several transmission zeros are introduced to improve passband isolation and stopband rejection. The proposed filter was designed, simulated, fabricated, and experimentally tested. Measured and simulated results show good agreement, making the proposed filter suitable for modern multi-standard wireless communication systems.

2. DESIGN AND MODELING FRAMEWORK FOR RESONATORS

This study investigates two types of dual-mode stepped-impedance resonators (SIRs), namely, a short-ended stepped-impedance resonator (SE-SIR) and an open-ended stepped-impedance resonator (OE-SIR), to achieve the desired resonances at 1.56, 2.5, 3.5, and 5.2 GHz. The proposed resonators are defined by the impedance parameters (Z_1), (Z_2), (Z_3) and the corresponding electrical lengths ($\theta_1, \theta_2, \theta_3, \theta_4, \theta_5, \theta_6, \theta_7, \theta_8$) as shown in Figs. 1(a) and 3(a). Their symmetric arrangements enable studying their resonance characteristics using even-odd mode decomposition. The obtained resonance conditions were then used to determine the electrical parameters and physical dimensions of the proposed resonators.

The equivalent circuit in Fig. 1(b) is obtained by applying the symmetry plane as an electrical boundary condition in the odd-mode analysis. The impedance sections Z_1, Z_3 and electrical lengths, θ_1 and θ_3 of the SE-SIR configuration control the odd-mode resonance. The resonator structure for the even-mode equivalent circuit in Fig. 1(c) can also be regarded as a stepped-impedance resonator (SIR). Under these excitation conditions, the loaded stub is in the resonant path and adds to the structure's effective electrical length.

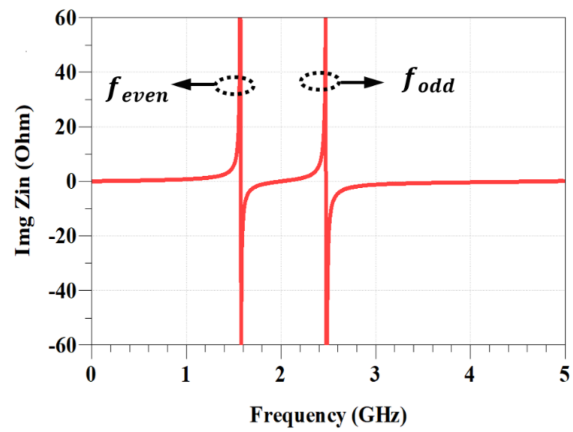

FIGURE 2. The proposed SE-SIR resonator's optimized geometry and dimensional parameters ($\ell_1 = 8.3$ mm, $\ell_2 = 2.7$ mm, $\ell_3 = 2.6$ mm, $\ell_4 = 2.0$ mm, $\ell_5 = 2.0$ mm, $W_1 = 0.5$ mm, $W_2 = 1.0$ mm, $W_3 = 1.5$ mm, $g_{c1} = 0.6$ mm, $D = 0.2$ mm) and the simulated Im(Z_{in}) response were used to verify the even- and odd-mode resonance behavior.

The odd-mode resonance condition and the corresponding electrical-length relation of the SE-SIR resonator are derived based on Eqs. (1) and (2), respectively

$$\tan\theta_1 \cdot \tan\theta_3 = Y_1/Y_3 = Z_3/Z_1 = R_Z \quad (1)$$

$$\theta_T = 2(\theta_1 + \theta_3) < \pi \quad (2)$$

where the electrical length of resonating sections is represented by (θ) and the impedance ratio by (R_Z).

Thus, even-mode resonance characteristics are obtained using transmission-line theory, and resonant frequencies are calculated using the following expressions [20]:

$$\tan(\theta_1+\theta_2+\theta_4) \cdot \tan\theta_3 = Y_1/Y_3 = Z_3/Z_1 = R_Z \quad (3)$$

$$\theta_T = (\theta_1+\theta_2+\theta_4 + \theta_3) < \pi \quad (4)$$

This design's loaded section satisfies the condition ($2Z_2 = Z_1$), simplifying analytical formulation.

These are resonance conditions for design flexibility of a resonant spectrum. This allows the resonant frequencies to be accurately distributed and independently controlled. The pro-

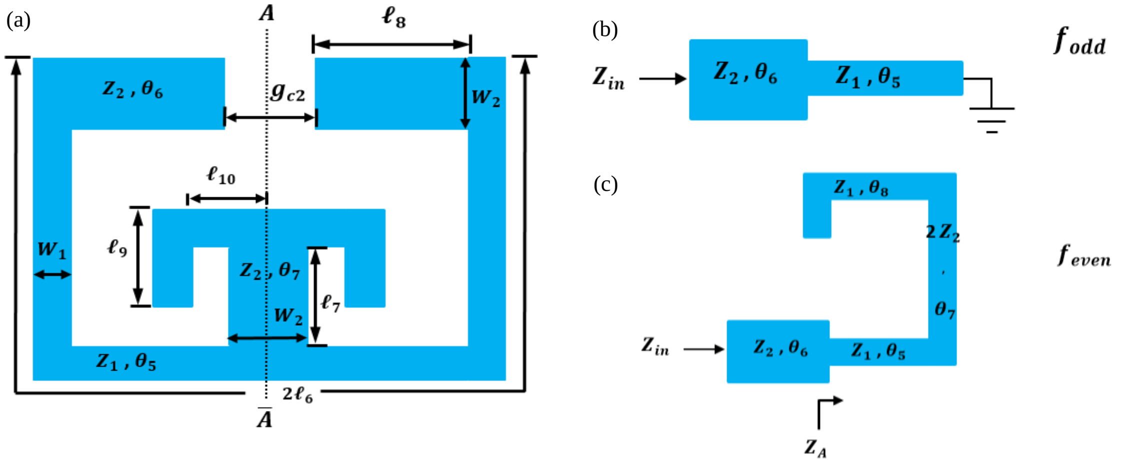

FIGURE 3. The suggested OE-SIR resonator's architecture and modal representation are as follows: (a) Physical structure, (b) odd-mode equivalent circuit, and (c) even-mode equivalent circuit.

posed resonators were implemented using a Rogers RO4360 substrate with a relative dielectric constant of ($\varepsilon_{r1\&2} = 6.15$) and thicknesses of ($h = 0.3$, $h_2 = 0.508$) mm. The impedance ratio ($R_Z = 0.3$) for the SE-SIR corresponds to $Z_1 = 69\,\Omega$, $Z_2 = 34.5\,\Omega$, and $Z_3 = 20.7\,\Omega$, respectively. Odd-mode resonance was achieved at a frequency of 2.5 GHz with a total electrical length of $\theta_T = 126°$, where $\theta_1 = 48°$ and $\theta_3 = 15°$. The design process is described in [20]. The even-mode resonance at 1.56 GHz was obtained with $\theta_T = 66°$ while meeting the requirements ($\theta_1 = 30°$, $\theta_2 = 9°$, $\theta_3 = 12°$, $\theta_4 = 15°$). Fig. 2 shows the simulated imaginary part of the input impedance of the proposed SL-SIR, which validates the creation of the desired even- and odd-mode resonances at 1.56 and 2.5 GHz, respectively.

Similarly, Fig. 3(b) illustrates that the odd-mode response of the OE-SIR is represented by impedance sections Z_1 and Z_2, which have electrical lengths θ_5 and θ_6, respectively. The resonator construction of the even-mode equivalent circuit in Fig. 3(c) can alternatively be viewed as a stepped-impedance resonator (SIR).

Odd-mode resonance characteristics of the OE-SIR resonator can be described using the following formulas:

$$\tan\theta_5 \cdot \tan\theta_6 = Y_1/Y_2 = Z_2/Z_1 = R_Z \quad (5)$$

$$\theta_T = 2(\theta_5 + \theta_6) < \pi \quad (6)$$

Derived equations offer a mathematical basis for determining odd-mode resonances in both resonator designs.

Furthermore, the even-mode resonance condition of the OE-SIR resonator is defined as [20]:

$$Z_{in} = Z_2 \cdot \frac{Z_A + jZ_2 \tan\theta_T}{Z_2 + jZ_A \tan\theta_T}$$

$$Z_A = -jZ_1 \cot\theta_A \quad (7)$$

$$\theta_A = (\theta_5 + \theta_7 + \theta_8)$$

$$\theta_T = (\theta_A + \theta_6) \quad (8)$$

The impedance ratio ($R_Z = 0.3$) for the SE-SIR corresponds to $Z_1 = 69\,\Omega$, $Z_2 = 34.5\,\Omega$, respectively. The OE-SIR achieved the requisite odd-mode resonance at 3.5 GHz with a total electrical length of $\theta_T = 132°$, with $\theta_5 = 54°$ and $\theta_6 = 12°$. The desired even-mode resonance at 5.2 GHz was achieved with a total electrical length of $\theta_T = 144°$, where $\theta_5 = 81°$, $\theta_6 = 20°$, $\theta_7 = 18°$, $\theta_8 = 25°$, and $\theta_A = 124°$. We verified the proposed analytical model through full-wave electromagnetic simulations using an Advanced Design System (ADS) simulator [21]. The simulated input-impedance response in Fig. 4 confirms the successful stimulation of intended resonant modes, with good agreement with theoretical expectations.

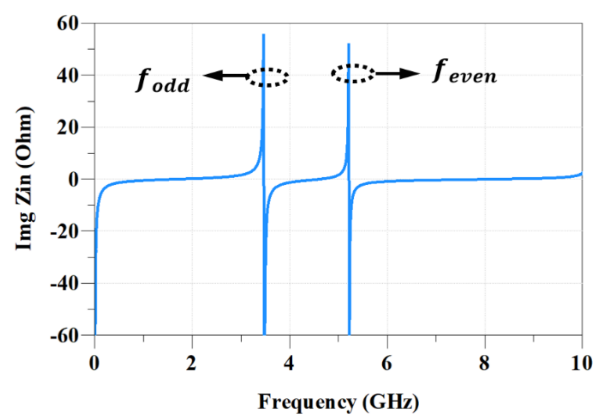

FIGURE 4. The OE-SIR resonator dimensions ($\ell_6 = 6.85$ mm, $\ell_7 = 1.6$ mm, $\ell_8 = 1.7$ mm, $\ell_9 = 1.15$ mm, $\ell_{10} = 0.95$ mm, $W_1 = 0.5$ mm, $W_2 = 1.0$ mm, $g_c = 0.8$ mm, $D = 0.2$ mm) and the accompanying simulated imaginary input-impedance response confirm the created dual-mode resonances.

3. QUAD-BAND HYBRID SE-SIR/OE-SIR FILTER CONFIGURATION

3.1. OE-SIR and SE-SIR Dual-band Filter Development

The proposed SE-SIR and OE-SIR resonators were implemented to realize two dual-band bandpass filters, which formed lower- and upper-frequency filtering sections of the final quad-band structure, following the resonator synthesis procedure de-

TABLE 1. Optimized in terms of physical dimensions are the dual-band filters SE-SIR and OE-SIR.

Substrate	Filter 1 (1.56/2.5) GHz		Filter 2 (3.5/5.2) GHz	
	Lengths (mm)	Widths & Gaps (mm)	Lengths (mm)	Widths & Gaps (mm)
Grounded substrate Rogers Ceramic RO4360 Dielectric constant $\varepsilon_{r1} = 6.15$ Thickness $h_1 = 0.3$ mm	$\ell_1 = 8.1$, $\ell_2 = 2.5$, $\ell_3 = 2.5$, $\ell_4 = 1.75$, $\ell_5 = 1.8$.	$W_1 = 0.5$, $W_2 = 1.0$, $W_3 = 1.5$, $g_{c1} = 0.6$, $D = 0.2$, $S_1 = 0.4$.	$\ell_6 = 6.6$, $\ell_7 = 1.5$, $\ell_8 = 1.6$, $\ell_9 = 1.15$, $\ell_{10} = 0.92$.	$W_1 = 0.5$, $W_2 = 1.0$, $g_{c2} = 0.8$, $S_1 = 0.4$.
Ungrounded substrate Rogers Ceramic RO4360 Dielectric constant $\varepsilon_{r2} = 6.15$ Thickness $h_2 = 0.508$ mm	$\ell_{w1} = 3$, $\ell_{w2} = 1.9$, $\ell_{w5} = 11$, $S_2 = 0.2$.	$W_1 = 0.5$, $W_3 = 1.5$, $W_5 = 1.4$, $W_p = 1.0$.	$\ell_{w3} = 1.0$, $\ell_{w4} = 1.4$, $\ell_{w6} = 5.5$.	$W_1 = 0.5$, $W_2 = 1.0$, $W_6 = 1.2$, $W_p = 1.0$.

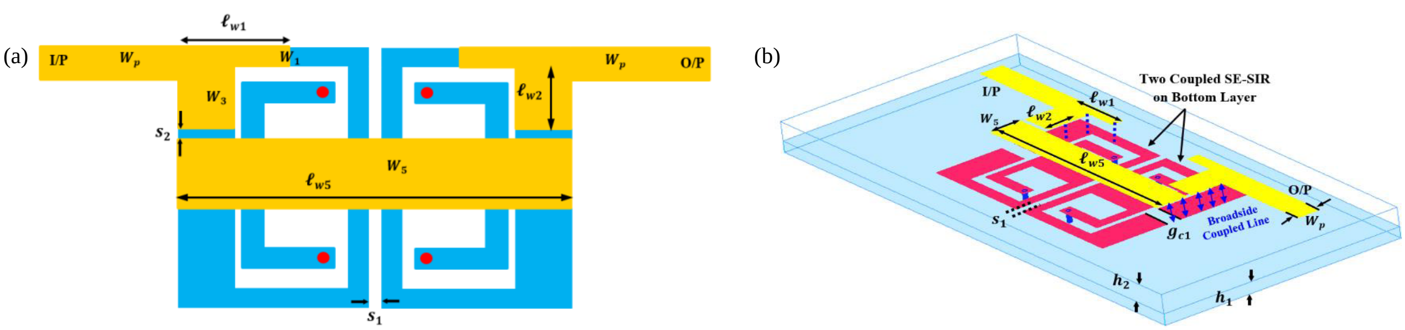

FIGURE 5. (a) The dual-band SE-SIR filter's geometry and multilayer broadside-coupled construction use two coupled short-ended stepped-impedance resonators and (b) a three-dimensional representation of the proposed filter.

scribed in Section 2. Both filters were designed on Rogers RO4360 substrates ($\varepsilon_{r1\&2} = 6.15$, $h = 0.3$ mm, $h_2 = 0.508$ mm) using a multilayer broadside-coupled design. The resonators were etched on the grounded substrate and excited by a feeding network placed on a separate top layer. This configuration provides independent control of resonance and coupling properties, increasing flexibility for bandwidth tuning and impedance matching while preserving compact circuit dimensions and resonance conditions expected by odd- and even-mode analyses.

Figure 5 shows the first dual-band filter built by combining two identical SE-SIR resonators. The resonators were placed symmetrically on the grounded layer with a coupling gap S_1 between them. The electromagnetic coupling between the resonators directly determines the coupling coefficient and bandwidth properties of the resulting passbands. At the same time, input and output signals were fed using broadside-coupled microstrip lines on the top substrate. The coupling between the resonators is mainly magnetic; however, this configuration produces capacitive coupling between the feeding network and the resonators. This coupling mechanism efficiently excites even- and odd-mode resonances and enhances the filtering performance.

The resonator dimensions obtained by the analytical synthesis described in Section 2 were converted into practical physical parameters using full-wave electromagnetic simulation and then optimized to consider effects of coupling interactions, fringing fields, and discontinuities related to the microstrip implementation, as listed in Table 1. As predicted by the resonance analysis, the simulated SE-SIR filter generated two passbands at 1.56 and 2.5 GHz, as shown in Fig. 6, corresponding to the even- and odd-mode resonances, respectively. The filter realized fractional bandwidths of 5.26% and 6.16%, return losses of 20.83 dB and 2373 dB, and insertion losses of 0.33 dB and 0.25 dB, respectively. Additionally, the response has better out-of-band rejection, stable transmission properties, and good suppression of higher-order resonances, confirming the applicability of the SE-SIR resonator for low-frequency, dual-band filtering applications and the proposed design method.

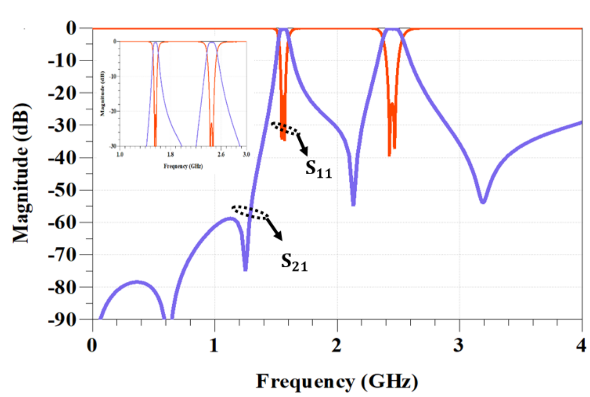

FIGURE 6. The suggested dual-band SE-SIR filter's simulated scattering characteristics (S_{11} and S_{21}) show passbands at 1.56 and 2.5 GHz.

TABLE 2. The final optimized geometrical parameters of the hybrid SE-SIR/OE-SIR quad-band filter.

Substrate	Filter 1 (1.56/2.5) GHz		Filter 2 (3.5/5.2) GHz	
	Lengths (mm)	Widths & Gaps (mm)	Lengths (mm)	Widths & Gaps (mm)
Grounded substrate Rogers Ceramic RO4360 Dielectric constant $\varepsilon_{r1} = 6.15$ Thickness $h_1 = 0.3$ mm,	$\ell_1 = 8.1$, $\ell_2 = 2.5$, $\ell_3 = 2.5$, $\ell_4 = 1.75$, $\ell_5 = 1.8$.	$W_1 = 0.5$, $W_2 = 1.0$, $W_3 = 1.5$, $g_{c1} = 0.6$, $D = 0.2$, $S_1 = 0.4$ $S_2 = 0.2$.	$\ell_6 = 6.6$, $\ell_7 = 1.5$, $\ell_8 = 1.6$, $\ell_9 = 1.15$, $\ell_{10} = 0.92$.	$W_1 = 0.5$, $W_2 = 1.0$, $g_{c2} = 0.8$, $S_1 = 0.4$ $S_2 = 0.2$.
Ungrounded substrate Rogers Ceramic RO4360 Dielectric constant $\varepsilon_{r2} = 6.15$ Thickness $h_2 = 0.508$ mm	$\ell_{w1} = 4.2$, $\ell_{w2} = 1.9$, $\ell_{w5} = 11.0$.	$W_1 = 0.5$, $W_3 = 1.5$, $W_5 = 1.4$, $W_p = 1.0$.	$\ell_{w3} = 3.7$, $\ell_{w4} = 2.2$, $\ell_{w6} = 7.0$.	$W_1 = 0.5$, $W_2 = 1.0$, $W_6 = 1.2$, $W_p = 1.0$.

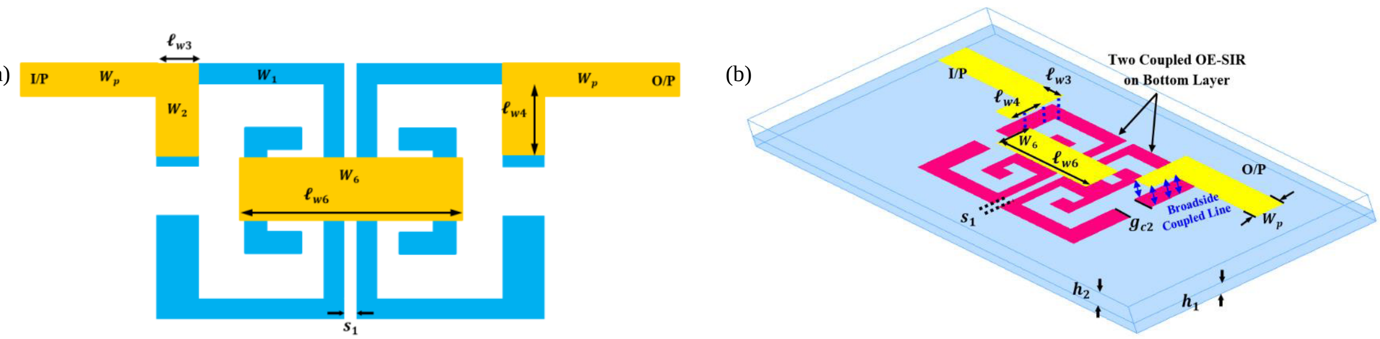

FIGURE 7. (a) The dual-band OE-SIR filter's geometry and multilayer broadside-coupled construction use two coupled open-ended stepped-impedance resonators, and (b) a three-dimensional representation of the proposed filter.

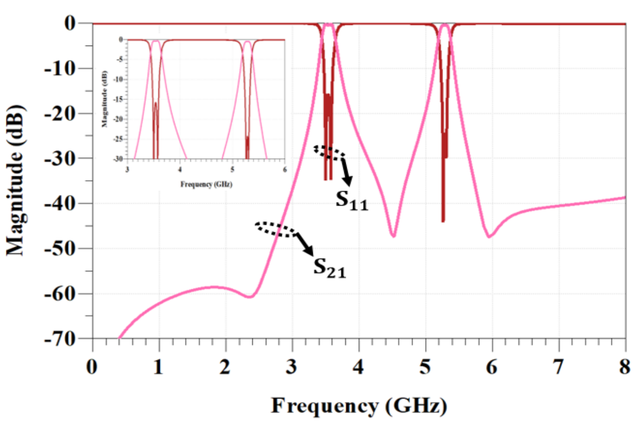

FIGURE 8. The simulation results show that the upper-band resonances at 3.5 and 5.2 GHz are activated by the OE-SIR filter.

For the upper-frequency filtering part, a second dual-band filter was designed based on the proposed OE-SIR resonator. The same multilayer feeding arrangement and coupling method were used, and only updated resonator parameters were described. Fig. 7 shows the shape of the matching filter, and Table 1 lists optimized dimensions. The coupling distance S_1 between the resonator pair is selected to obtain the desired bandwidth and selectivity. Fig. 8 presents two passbands centered at 3.5 and 5.2 GHz, which are well generated by the constructed OE-SIR filter. The resonance frequencies predicted by the modal analysis are in good agreement with the simulated results. The resonator's open-ended design provides a finer passband assignment and better resonance control at upper frequencies. The resultant response shows return losses of 15.82 and 24.32 dB, insertion losses of 0.34 and 0.45 dB, and fractional bandwidths of 6.00% and 3.46%, respectively, along with crisp transition characteristics and good frequency selectivity. The two fabricated dual-band filters and the SE-SIR filter that generates lower-frequency passbands at 1.56 and 2.5 GHz effectively yield four independently controlled resonances.

3.2. Implementation and Performance Analysis of Hybrid Quad-Band Filter

We tested the performance of separate dual-band filters and then combined into a common multilayer platform to create the proposed quad-band bandpass filter. Fig. 9 shows the final structure. The integration process couples the low-frequency filtering part based on SE-SIR resonators with the high-frequency filtering part based on OE-SIR resonators through a shared feeding network and a coupled space S_2. With this method, it is possible to generate four passbands concurrently while preserving resonant characteristics of each set of resonators. The operation of the proposed filter can be explained by the contribution of each pair of resonators. The first and second passbands are centered at 1.56 and 2.5 GHz with SE-SIR resonators, and the third and fourth passbands are at 3.5 and 5.2 GHz with OE-SIR resonators. The interaction between adjacent passbands is small because each family of resonators has its own frequency range. The improved quad-band filter was assessed using a

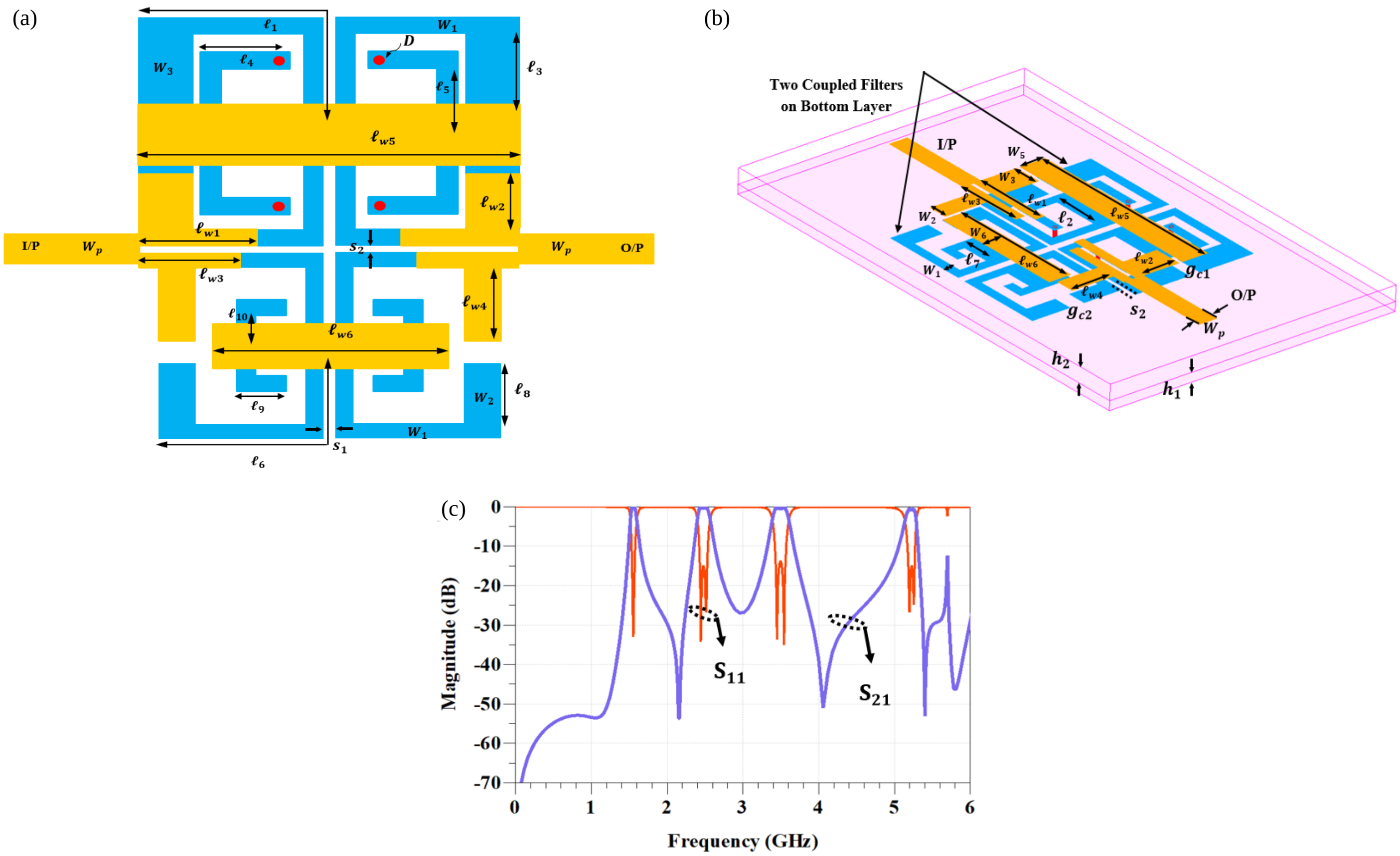

FIGURE 9. (a) The proposed hybrid quad-band filter, which combines the OE-SIR and SE-SIR filtering sections into one multilayer feeding structure, (b) a three-dimensional representation of the suggested final filter, and (c) its simulated S-parameter responses (S11 and S21).

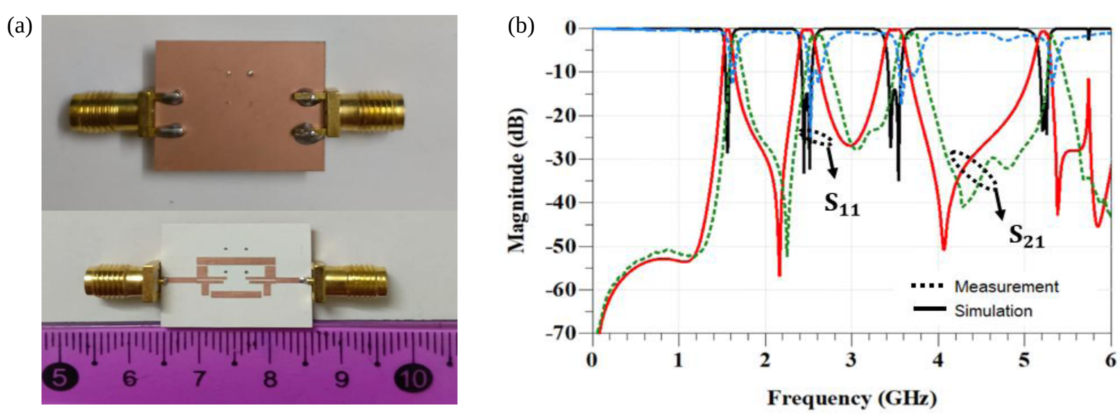

FIGURE 10. Experimental verification of the proposed quad-band filter. (a) Photograph of the prototype manufactured and (b) comparison of simulated and measured S-parameter responses.

full-wave electromagnetic simulator, with dimensions shown in Table 2.Fig. 9(b) presents simulated scattering parameters. Four passbands were effectively established at 1.56, 2.5, 3.5, and 5.2 GHz. Simulated return losses were 25.6, 15.05, 13.94, and 18.6 dB, with corresponding insertion losses of 0.29, 0.37, 0.43, and 0.68 dB, respectively. Moreover, multiple transmission zeros are created at the passband margins, providing strong skirt selectivity and significant out-of-band suppression. The suggested filter has a small dimension of $0.12\lambda_g \times 0.13\lambda_g$, a compact size, flexible frequency allocation, and high filtering performance.

Fig. 10(a) shows the fabricated prototype, and Fig. 10(b) shows a comparison of measured and simulated scattering properties. The measured and simulated results are in good agreement, confirming the proposed hybrid SE-SIR/OE-SIR configuration. The small discrepancies are mostly due to manufacturing tolerances, conductor losses, variations in dielectric parameters, and the effect of SMA connections. The results obtained show the effectiveness of the proposed design and verify

TABLE 3. Comparative analysis of published multiband bandpass filters and the suggested multilayer quad-band filter.

Ref.	Resonator Structure	Operating Frequencies (GHz)	IL (dB)	RL (dB)	FBW (%)	TZs	Area (λ_g^2)	Technology
[2]	SSLSIR + Embedded SIR	2.45/3.50/5.20	< 2.0	> 15	9.6/13.1/7.9	4	0.0486	Microstrip Triple-Band SIR
[16]	Multilayer Dual-Mode Resonator	1.90/3.50	< 1.0	> 20	3.5/2.8	4	0.0083	Multilayer DMR
[10]	Dual Coupling Path Resonator	3.50/5.80	< 2.0	> 19	0.8/1.0	2	0.0273	Ultra-Narrowband BPF
[5]	Coupled Resonators	3/6.3	0.3/1.3	> 15	8.33/1.9	7	0.056	Coupled-Line Resonator (Microstrip)
[6]	Quarter-Wave Dual-Mode Resonator	0.85/1.57	0.98/1.11	> 15	16.84/3.5	2	0.0095	Dual-Mode Microstrip
This Work	**Dual-Mode SE-SIR + OE-SIR**	**1.56/2.50/3.50/5.20**	**0.29/ 0.26/ 0.43/ 0.66**	**28.65/ 15.05/ 14.04/ 17.3**	**7.05/ 6.4/ 5.71/ 2.5**	**6–8**	**0.0156**	**Multilayer Broadside-Coupled SIR**

its suitability for tiny multiband wireless communication applications. To further evaluate effectiveness, the performance of the simulated proposed design was compared with that of previously reported bandpass filters in operating frequency, return loss, insertion loss, circuit size, fractional bandwidth, and implementation technology. Table 3 shows the results.

The comparison demonstrates desired trade-off among circuit compactness, frequency selectivity, and passband allocation flexibility, while guaranteeing proper filtering performance in all operating bands. Other advantages of the multilayer broadside-coupled design are better passband selectivity, flexible frequency allocation, and better coupling controllability. SE-SIR and OE-SIR resonators are independently tunable. The proposed filter is a compact and efficient solution for modern multi-band wireless communication systems that require quad-band operation.

4. CONCLUSION

In this study, a novel hybrid SE-SIR/OE-SIR quad-band bandpass filter was designed, fabricated, and experimentally verified. Using the modal features of two families of dual-mode resonators in a multilayer broadside-coupled system, we achieve four independently controllable passbands at 1.56, 2.5, 3.5, and 5.2 GHz. By producing a large number of transmission zeros, the proposed structure can achieve a compact size, flexible frequency distribution, and enhanced selectivity. The analytical design technique and full-wave electromagnetic optimization procedure were validated using the manufactured prototype, which showed high agreement between measured and simulated results. The suggested design offers four operational passbands within a small size of $0.0158\lambda_g{}^2$, in contrast to previously reported dual- and multi-band filters. 7.05%, 6.4%, 5.71%, and 2.50% are the appropriate fractional bandwidths. The suggested dual-mode SE-SIR/OE-SIR topology offers a competitive mix of multiband capabilities and small circuit size, as shown by the comparison with current designs, and is thus ideally suited for future multiband wireless communication applications.

ACKNOWLEDGEMENT

The authors declare that no funds, grants, or other support were received during the preparation of this manuscript.

REFERENCES

[1] Tahaİmeci, S., B. Tütüncü, F. Bešlija, and L. Herceg, "Microstrip filters based on open stubs and SIR for high frequency and ultra-wideband applications," *Journal of Engineering Research*, Vol. 10, No. 3, 212–223, Sep. 2022.

[2] Xu, K.-D., Y.-H. Zhang, D. Li, Y. Fan, J. L.-W. Li, W. Joines, and Q. H. Liu, "Novel design of a compact triple-band bandpass filter using short stub-loaded SIRs and embedded SIRs structure," *Progress In Electromagnetics Research*, Vol. 142, 309–320, 2013.

[3] Hu, C., X.-Z. Xiong, Y.-L. Wu, and C. Liao, "Design dual-mode bandpass filters based on symmetrical T-shaped stub-loaded stepped-impedance resonators with high frequencies selectivity," *Progress In Electromagnetics Research B*, Vol. 55, 325–345, 2013.

[4] Zhang, Q., C. Chen, W. Chen, J. Ding, and H. Zhang, "Novel cross-coupled dual-band bandpass filters with compact size based on dual-mode isosceles right-angled triangular resonators," *IEEE Transactions on Microwave Theory and Techniques*, Vol. 69, No. 6, 3037–3047, Jun. 2021.

[5] Yahya, S. I., A. Rezaei, and Y. A. Khaleel, "Design and analysis of a wide stopband microstrip dual-band bandpass filter," *ARO-The Scientific Journal of Koya University*, Vol. 9, No. 2, 83–90, 2021.

[6] Basit, A., M. I. Khattak, M. Al-Hasan, J. Nebhen, and A. Jan, "Design and analysis of a compact GSM/GPS dual-band bandpass filter using T-shaped resonator," *Journal of Electromagnetic Engineering and Science*, Vol. 22, No. 2, 138–145, 2022.

[7] Hammed, R. T. and S. M. Abbas, "Small dual narrowband BPF with ultra-rejection band using grounded stepped-impedance resonator," *IETE Journal of Research*, Vol. 69, No. 5, 2811–2816, 2023.

[8] Liu, J. and D. Psychogiou, "Dual-band bandpass filters using 3D printed dual-mode nested spherical resonators," *IEEE Access*, Vol. 12, 64 439–64 445, 2024.

[9] Li, Y., J. Ni, S. Li, Q. Han, J. Tian, N. Li, and T. Ma, "Miniaturized dual-band bandpass filter with closely spaced passbands and wide stopband," *Frontiers in Physics*, Vol. 13, 1637651, 2025.

[10] Mu, R., Y. Wu, L. Pan, W. Zhao, and W. Wang, "A miniaturized low-loss switchable single- and dual-band bandpass filter," *International Journal of RF and Microwave Computer-Aided Engineering*, Vol. 2023, 9025980, 2023.

[11] Karimi, G., Y. Pourasad, A. Lalbakhsh, H. Siahkamari, and B. Mohamadzade, "Design of a compact ultra-narrow band dual band filter for WiMAX application," *AEU — International Journal of Electronics and Communications*, Vol. 110, 152827, 2019.

[12] Shen, G., W. Feng, W. Che, Y. Shi, and Y. Shen, "Millimeter-wave dual-band bandpass filter with large bandwidth ratio using GaAs-based integrated passive device technology," *IEEE Electron Device Letters*, Vol. 42, No. 4, 493–496, 2021.

[13] Kumar, K. V. P., V. K. Velidi, A. A. Althuwayb, and T. R. Rao, "Microstrip dual-band bandpass filter with wide bandwidth using paper substrate," *IEEE Microwave and Wireless Components Letters*, Vol. 31, No. 7, 833–836, 2021.

[14] Najafi, M. and A. R. Hazeri, "Microstrip dual-narrowband bandpass filter with independent passbands," *Wireless Personal Communications*, Vol. 119, No. 4, 3503–3516, 2021.

[15] Wei, F., C. Y. Zhang, C. Zeng, and X. W. Shi, "A reconfigurable balanced dual-band bandpass filter with constant absolute bandwidth and high selectivity," *IEEE Transactions on Microwave Theory and Techniques*, Vol. 69, No. 9, 4029–4040, 2021.

[16] Wu, L., Y. Wu, X. Cheng, R. Huang, and W. Wang, "Design of dual-mode dual-band filter based on multilayer groove gap waveguide," *AEU — International Journal of Electronics and Communications*, Vol. 173, 154975, 2024.

[17] Hammed, R. T. and D. G. Hammood, "Miniaturized dual-band bandpass filter using multilayered dual-mode resonator," *Diyala Journal of Engineering Sciences*, Vol. 11, No. 1, 2018.

[18] Hammed, R. T., "Miniaturized dual-band bandpass filter using E-shape microstrip structure," *AEU — International Journal of Electronics and Communications*, Vol. 69, No. 11, 1667–1671, 2015.

[19] Yang, L., M. Malki, and R. Gómez-García, "Multilayer dual-band bandpass filter using microstrip-to-slotline transitions and transversal signal-interference microstrip lines," in *2024 IEEE Radio and Wireless Symposium (RWS)*, 79–82, San Antonio, TX, USA, 2024.

[20] Makimoto, M. and S. Yamashita, *Microwave Resonators and Filters for Wireless Communication: Theory, Design and Application*, Springer Science & Business Media, 2001.

[21] Alto, C. P., Advanced Design System (ADS), Keysight Technologies, USA, 2016.